

1 **Conservation tillage increases corn and soybean water productivity across the Ohio River**
2 **Basin**

3 Yawen Huang¹, Bo Tao¹, Xiaochen, Zhu^{1, 2}, Yanjun Yang¹, Liang Liang³, Lixin Wang⁴, Pierre-
4 Andre Jacinthe⁴, Hanqin Tian⁵, and Wei Ren^{1*}

5 ¹Department of Plant & Soil Sciences, College of Agriculture, Food, and Environment,
6 University of Kentucky, Lexington, KY 40546, USA

7 ²School of Geography and Remote Sensing, Nanjing University of Information Science and
8 Technology, Nanjing, China

9 ³Department of Geography, College of Arts & Sciences, University of Kentucky, KY 40506,
10 USA

11 ⁴Department of Earth Sciences, Indiana University–Purdue University Indianapolis, Indianapolis,
12 IN 46202, USA

13 ⁵International Center for Climate and Global Change Research and School of Forestry and
14 Wildlife Sciences, Auburn University, Auburn, AL 36849, USA

15

16 **Correspondence:**

17 Wei Ren, wei.ren@uky.edu

18

19 *To be submitted to Agricultural Water Management*

20 March 2021

This is the author's manuscript of the article published in final edited form as:

Huang, Y., Tao, B., Xiaochen, Z., Yang, Y., Liang, L., Wang, L., Jacinthe, P.-A., Tian, H., & Ren, W. (2021). Conservation tillage increases corn and soybean water productivity across the Ohio River Basin. *Agricultural Water Management*, 254, 106962. <https://doi.org/10.1016/j.agwat.2021.106962>

21 **Abstract**

22 Optimizing agricultural management practices is imperative for ensuring food security and
23 building climate-resilient agriculture. The past several decades have witnessed the emergence of
24 conservation tillage practices to combat soil erosion and degradation. However, the effects of
25 conservation tillage on crop water productivity (CWP) remain uncertain, especially from a
26 regional-scale perspective. Here, we used an improved process-based agroecosystem model
27 (DLEM-Ag) to quantify the long-term effects of conservation tillage (e.g., no-tillage, NT;
28 reduced tillage, RT) on CWP (defined as the ratio of crop productivity to evapotranspiration) of
29 corn and soybean across the Ohio River Basin during 1979-2018. Our results revealed an
30 average increase of 2.8% and 8.4% in CWP for corn and soybean, respectively, under the NT
31 adoption scenario. Compared to the conventional tillage scenario, NT and RT would enhance
32 CWP, primarily due to reductions in evapotranspiration, particularly evaporation. Further
33 analysis suggested that, although NT and RT may decrease surface runoff, these practices could
34 also increase subsurface drainage and nutrient loss from corn and soybean farmland via leaching.
35 These results indicate that conservation tillage should be complemented with additional water
36 and nutrient management practices to enhance soil water retention and optimize nutrient use in
37 the region's cropland. Our findings also provide unique insights into optimizing management
38 practices for other areas where conservation tillage is widely applied.

39 **Keywords:** Conservation tillage, Crop water productivity (CWP), No-tillage, Ohio River Basin
40 (ORB), Process-based agroecosystem model

41 **Abbreviations**

42	CWP	crop water productivity
43	CT	conventional tillage
44	ET	evapotranspiration
45	GPP	gross primary productivity
46	NT	no-tillage
47	RT	reduced tillage
48	ORB	Ohio River Basin

49 **1. Introduction**

50 Water deficits and surpluses represent the greatest challenge facing rain-fed agriculture
51 worldwide (Shekhar and Shapiro, 2019). Increasing drought and extreme rainfall events have
52 already caused significant impacts on water resources and food security globally (Daryanto et al.,
53 2017a; Drum et al., 2017; Li et al., 2019). Adaptation of management practices is critical to
54 improve water resource use efficiency and build climate-resilient agricultural systems (Tian et al.,
55 2018). In that regard, conservation tillage has emerged as a promising option that can help
56 conserve soil moisture and reduce soil erosion, thus alleviating the impact of rainfall deficit on
57 crop yields (Busari et al., 2015; Holland, 2004; Phillips et al., 1980). However, its effects on
58 regional crop water productivity (CWP, defined as the ratio of crop carbon gain to water
59 consumption, Van Halsema and Vincent, 2012) have not yet been fully investigated.

60 Conservation tillage refers to any tillage system with a seedbed preparation technique in
61 which at least 30% of the soil surface is covered by crop residues (Lal et al., 2017), including no-
62 tillage (NT), reduced tillage (RT), mulch tillage, and ridge tillage. Compared to conventional
63 tillage (CT), conservation tillage decreases soil disturbance and leaves more crop residues on the
64 soil surface. Some studies have reported the positive effects of conservation tillage on CWP

65 across different agroecosystems (Cantero-Martínez et al., 2007; Jabro et al., 2014; Li et al., 2018;
66 Su et al., 2007; Tang et al., 2015). However, other studies have found no effect of conservation
67 tillage on CWP or even lower CWP than CT (Guan et al., 2015; Irmak et al., 2019; Liu et al.,
68 2013). With the recognition that the effects of conservation tillage on CWP involve alteration of
69 soil properties and soil water dynamics in the rhizosphere (O'Brien and Daigh, 2019), these
70 variable results likely reflect not only the direct effect of a tillage practice but also its interactions
71 with climate, soil type, land management history, and cropping systems (Strudley et al., 2008).
72 Failure to account for these differences could lead to uncertainties in regional assessments of the
73 effectiveness of conservation tillage.

74 Previous studies examining linkages between conservation tillage and CWP have largely
75 in arid/semi-arid regions (Jalal et al., 2014; Yang et al., 2018; Irmak et al., 2019). Less attention
76 has been paid to how conservation tillage affects crop water use in humid areas. These areas face
77 more synergistic effects of water and nutrient supply and are more vulnerable to changes in
78 rainfall (Wuebbles et al., 2017). Although several studies have used remote sensing products
79 (e.g., MODIS GPP and ET) to quantify large-scale variation in CWP (Ai et al., 2020; Lu and
80 Zhuang; 2010), they usually generated results for all croplands but did not provide crop-specific
81 CWP estimates. Moreover, regional and global CWP simulations have generally ignored tillage
82 effects, in part because of the under-representation of tillage processes in global ecosystem
83 models (Tian et al., 2015; Lutz et al., 2019). It is essential to adopt an integrated approach that
84 links process-based agricultural models with ground and satellite observation data to advance
85 predictive understanding of tillage effects on regional CWP.

86 Located in the Eastern Corn Belt (Fig. 1), the Ohio River Basin (ORB) is a highly
87 agricultural watershed with almost 98% of its croplands supporting corn and soybean production

88 (according to the 2018 National Cropland Data Layer). The agricultural landscape in the ORB is
89 susceptible to soil erosion due to heavy rains (Drum et al., 2017). Conservation tillage has been
90 promoted as a tool to address soil erosion in this region. Introduced to the ORB region in the
91 1960s and encouraged by agricultural extension agencies, conservation tillage has steadily grown
92 in adoption during the past several decades (Franklin and Bergtold, 2020). More than 60% of
93 corn and almost 80% of soybean in the ORB are grown under different forms of conservation
94 tillage (CTIC, 2018). The spread of conservation tillage systems in the ORB justifies the need to
95 assess its impact on water use for the dominant crops in the region. Long-term and spatially
96 explicit information on tillage practice effects is urgently needed to address questions of water
97 resource optimization and predicting food production and shortages in the context of climate
98 change. Therefore, the ORB provides an ideal context for a regional examination of these
99 questions using our proposed integrated approach.

100 Here we used a process-based agroecosystem model (DLEM-Ag) to quantify the
101 magnitude and spatiotemporal patterns of CWP across the ORB corn-soybean cropping system
102 for the period 1979-2018. We noticed that CWP has a long tradition among crop physiologists
103 that continue to call water use efficiency (WUE) (e.g., Bluemling et al., 2007; Perry, 2007).
104 WUE is defined as $WUE = [\text{product}] / [\text{water applied} / \text{water available}]$, representing an efficiency
105 parameter of water utilization at the farm/plot level, which is scale- and context-dependent (Van
106 Halsema and Vincent, 2012). We defined the CWP as the ratio of GPP and ET to investigate
107 coupled carbon assimilation and water consumption from an ecosystem perspective. Our specific
108 objectives were to 1) investigate the magnitude and long-term trends in CWP for corn and
109 soybean in the ORB, 2) quantify changes in CWP as affected by different tillage practices, and 3)
110 explore relationships between carbon and water fluxes in different tillage systems.

111

<Insert Figure 1>

112 **2. Materials and Methods**

113 **2.1 Description of the Study Area**

114 The ORB covers 421,966 km² within 11 states. The Ohio River starts at the Allegheny and the
115 Monongahela's confluence in Pittsburgh, Pennsylvania, and ends in Cairo, Illinois, where it
116 flows into the Mississippi River. The humid continental climate is prevalent in the upper half of
117 the basin, and a humid subtropical climate is dominant in the lower half of the basin. Annual
118 rainfall for different regions within the ORB ranges between 990 mm and 1473 mm. From 1979
119 to 2018, basin-wide annual rainfall averaged 1175 mm, with a coefficient of variation of 0.12.
120 Nearly half of the land area in the ORB is covered by forests, primarily secondary growth
121 deciduous trees. Cultivated cropland (~ 30%) is dominant in the northern and western sections of
122 the ORB, with corn and soybean being the major crops grown (Santhi et al., 2014).

123 The northern portion of the ORB is near the glacial margin during the Late Pleistocene. The
124 humid temperate climate and predominance of deciduous forests during the Holocene have led to
125 the formation of Alfisols across most of the basin. In the eastern and southeastern portions of the
126 basin, cropland soils are generally well-drained across various slope conditions (~57% well-
127 drained, Schilling et al., 2015). In contrast, croplands in the northern and northwestern portions
128 of the basin are characterized by poorly drained conditions with slopes often < 5%.

129 **2.2 Model description**

130 **2.2.1 The DLEM-Ag**

131 The agricultural module of the Dynamic Land Ecosystem Model (DLEM-Ag) is a highly
132 integrated process-based agroecosystem model. The DLEM-Ag is capable of simulating the daily
133 crop growth and exchanges of trace gases (CO₂, CH₄, and N₂O) between agroecosystems and the
134 atmosphere; and quantifying fluxes and storage of carbon, water, and nitrogen within
135 agroecosystems as affected by multiple factors such as climate, atmospheric CO₂, nitrogen
136 deposition, tropospheric ozone, land use and land cover change, and agriculture management
137 practices (e.g., harvest, rotation, irrigation, and fertilizer use). The model has been extensively
138 used to study crop production, soil organic carbon, and greenhouse gas emissions in
139 agroecosystems at regional and global scales. The detailed structure and processes of the model
140 have been well documented in previous work (e.g., Ren et al., 2011; Ren et al., 2012; Ren et al.,
141 2016; Ren et al., 2020; Tian et al., 2010; Tian et al., 2015; Zhang et al., 2018).

142 **2.2.2 Model representation of tillage effects**

143 We have recently incorporated a tillage sub-module in the DLEM-Ag model (Huang et al., 2020).
144 The implementation of tillage mainly focuses on two processes that are directly affected by
145 tillage: 1) the redistribution of surface residues with tillage practice and subsequent effects on
146 soil water dynamics and water-related processes; 2) the increase in decomposition rates. The
147 tillage effects are implemented in combination with residue management, as these management
148 practices are often interrelated (Strudley et al., 2008). Tillage incorporates surface residues into
149 the soil, altering the coverage of residues on top of the soil. Crop residues left on soil surface
150 intercept rainfall, facilitating water infiltration. Surface residues also serve as a barrier that

151 lowers soil evaporation and reduces water losses to the atmosphere. Therefore, crop residues
152 help maintain or improve soil moisture. Soil moisture affects primary production by regulating
153 the amount of available water for plants, and in turn, plant water uptake also changes soil
154 moisture. The tillage sub-module does not consider the direct effect of tillage on soil thermal
155 properties due to the scarcity of studies on soil thermal properties under different tillage regimes
156 (Blanco-Canqui and Ruis., 2018; O'Brien and Daigh, 2019). However, as soil thermal properties
157 are intimately associated with soil hydraulic properties in the DLEM-Ag, the tillage sub-module
158 indirectly affects soil temperature by changing soil water content.

159 **2.3 Input data**

160 **2.3.1 Climate, CO₂, and Nitrogen deposition**

161 The daily climate data used to drive the model were derived from the gridMET dataset at a
162 resolution of 4 km × 4 km covering the United States from 1979-2018 (Abatzoglou, 2013),
163 including maximum, minimum, and average temperature; precipitation; shortwave radiation;
164 wind; and relative humidity. The historical atmospheric CO₂ concentration dataset was obtained
165 from the Earth System Research Laboratory of NOAA (National Oceanic and Atmospheric
166 Administration, <https://www.esrl.noaa.gov/gmd/>). Gridded nitrogen deposition maps were
167 extracted from the North American Climate Integration and Diagnostics – Nitrogen Deposition
168 Version 1 (NACID-NDEP1) dataset (Hember, 2018).

169 **2.3.2 Crop rotation and crop phenology**

170 The crop rotation maps were generated by using the USDA-NASS Cropland Data Layer (CDL)
171 datasets. Following a similar approach by Panagopoulos et al. (2015) and Srinivasan et al. (2010),
172 we overlaid multi-year CDL information to produce crop rotation maps. This process resulted in

173 dominant corn-soybean or soybean-corn rotations for the cropland portion of the region. The
174 2018 CDL data showed that approximately 98% of croplands in the ORB were planted with corn
175 and soybean. Based on a three-year rotation pattern in the ORB from 2015 to 2017, we derived
176 eight cropland rotation types involving corn and soybean: 1) corn/soybean, 2)
177 corn/soybean/soybean, 3) corn/corn/soybean, 4) soybean/corn, 5) soybean/corn/corn, 6)
178 soybean/soybean/corn, 7) continuous corn, and 8) continuous soybean. These eight rotation types
179 constitute approximately 90% of all the three-year rotations that involve corn or soybean in the
180 ORB (Table. S1). Therefore, minor rotation types such as corn/soybean/wheat and
181 corn/corn/wheat were not included. We then aggregated the 30-m rotation information to
182 produce fractional rotation types at a spatial resolution of 4-km (Fig. 1).

183 The planting and harvesting dates for corn and soybean were derived using the 500-m crop
184 phenology dataset from Yang et al. (2020) combined with the CDL datasets. Specifically, we: 1)
185 calculated corn and soybean fractions in each 500-m grid cell; 2) overlaid the center of each 4-
186 km pixel on the 500-m phenology map to assign the index of the 500-m pixel to the nearest 4-km
187 pixel; 3) searched within 10 km around the center on the 4-km map to find the pixels with more
188 than 55% of corn or soybean (assuming that corn or soybean phenology information dominates
189 pixels with more than 55% coverage); 4) assigned the planting/harvesting date of corn and
190 soybean at the nearest pixel to the center of the 4-km pixel. For unassigned pixels, we replaced
191 the value with the most adjacent pixels. Overall, the planting date in the ORB was 97-177 (day
192 of the year) for both corn and soybean. The harvesting dates were 289-330 and 277-290 for corn
193 and soybean, respectively.

194 **2.3.3 Tillage and other agricultural management practices**

195 We obtained county-level ORB tillage information from the National Crop Residue Management
196 Survey (CRM) compiled by the Conservation Technology Information Center
197 (<https://www.ctic.org/>). The tabular data provides the acreages and percentages of five tillage
198 types adopted in all crops, including corn and soybean. For simplification, we grouped the five
199 major tillage types into three categories, i.e., no-tillage, reduced tillage (including ridge tillage,
200 mulch tillage, and reduced tillage), and conventional tillage. We used county acreages combined
201 with the CDL maps to estimate the spatial distribution of conventional and conservation tillage
202 for corn and soybean, assuming each pixel within a county has the same rates of the tillage-
203 specific area. We reconstructed annual tillage maps from 1979-2018 based on the CRM dataset
204 (1989-2011) and assumed that the tillage maps of other years are similar to the nearest year.
205 Moreover, we also generated three tillage maps with all the corn/soybean under a specific tillage
206 regime such as NT, RT, or CT for sensitivity analysis.

207 Crop-specific nitrogen fertilizer use data were derived from the USDA Economic
208 Research Service statistics on fertilizer use ([https://www.ers.usda.gov/data-products/fertilizer-
209 use-and-price.aspx](https://www.ers.usda.gov/data-products/fertilizer-use-and-price.aspx)), covering 1960-2018. A 4-km irrigation map was reconstructed based on the
210 MODIS irrigated agriculture dataset (2012) for the United States (MIRAD-US, Pervez and Brown,
211 2010).

212 **2.4 Model evaluation**

213 The DLEM-Ag model has been extensively calibrated and validated against both site-level and
214 regional-scale data (Ren et al., 2011, 2012, 2016, 2020; Tian et al., 2010; Zhang et al., 2018).
215 Because we used driving forces different from previous regional studies and mainly focused on

216 corn and soybean systems, we specifically calibrated and validated the simulated crop GPP and
217 ET against published results from cropland sites in the AmeriFlux Network
218 (<https://ameriflux.lbl.gov/>) within and close to the ORB region. One site is an agricultural field
219 on a corn-soybean rotation at the Fermi National Accelerator Laboratory-Batavia, Illinois (US-
220 IB1, 41.86° N, 88.22°W). The field has been farmed for more than 100 years, and the corn-
221 soybean rotation with conventional tillage was established in July 2005. Soil texture at this site is
222 silt clay loam in the topsoil and clay from in the subsoil. The other site was established in 1996 at
223 Bondville, Illinois (US-Bo1, 40.01°N, 88.29°W). The field is under continuous no-tillage with
224 alternating years of corn and soybean crops. Both sites have a typical humid continental climate
225 with hot, humid summers and cool to cold winters, and they are representative of the northern
226 central lowland. The model was calibrated using the first two-year data at each location and
227 validated against the available data for the remaining years. Our evaluation results showed a
228 general agreement between the simulated GPP and ET with measurements made at the flux
229 towers (Fig. 2a, b).

230 To evaluate the model performance at the regional level, we further compared simulated NPP
231 with survey and remote sensing products (Fig. 2c and 2d). The temporal pattern of crop NPP at
232 the basin level was evaluated against the historical crop NPP derived from crop yield records
233 reported by the USDA and derived from the Moderate Resolution Imaging Spectroradiometer
234 (MODIS) NPP product (MOD17A3). Specifically, the USDA crop yield records were converted
235 to NPP following the method from Prince et al. (2001) and Li et al. (2014):

$$236 \quad NPP = yield \times f_{mass} \times f_{dry} \times f_{carbon} \times (1 + RS)/HI$$

237 where yield is the crop yield in report unit by USDA inventory (bushel, pound, etc.), f_{mass} is a
238 factor to convert the raw yield data into a standard unit of biomass, f_{dry} is a factor to convert the
239 mass to dry biomass, f_{carbon} is a carbon content factor to convert the dry biomass to carbon (we
240 use 450 g C/kg), HI is the harvested index, and RS is the root/shoot ratio. More details can be
241 found in Li et al. (2014) and Ordóñez et al. (2020).

242 We overlaid the MODIS NPP maps with the CDL land cover data to extract corn and soybean
243 NPP from 2008 to 2017. The results showed that the simulated NPP was generally within the
244 range of survey-based NPP but relatively higher for corn and lower for soybean than those
245 estimated by MODIS. This discrepancy could be attributed partially to the light use efficiency
246 parameterization in the MODIS algorithm, which uses one light use efficiency value to represent
247 all crops (Turner et al., 2006; Bandaru et al., 2013). Our results are in agreement with previous
248 studies that MODIS NPP products tend to overestimate at low productivity sites and
249 underestimate at high productivity sites (Turner et al., 2005; Turner et al., 2006).

250 *<Insert Figure 2>*

251 **2.5 Model experimental design**

252 We designed four simulation scenarios to assess the magnitude and spatiotemporal patterns of
253 corn and soybean CWP (calculated as $CWP = GPP/ET$) during 1979-2018 and analyzed the
254 difference associated with various tillage systems (Table 1). The model simulation began with an
255 equilibrium run using 30-years (1979-2008) mean climate to develop the simulation boundary, in
256 which the year-to-year variations of carbon, nitrogen, and water pools in each grid were less than
257 0.1 g C/m²/yr, 0.1 mm H₂O/yr, and 0.1 g N m²/yr, respectively. Before the transient run, the
258 model was run for another 100 years for the spin-up to remove system fluctuations caused by the

259 shift from equilibrium to transient state, using climate data randomly selected from 1979-2008.
260 The baseline simulation scenario (S1) was designed to produce CWP close to reality and its
261 changes across the ORB. It was driven by historically varying tillage types and other input
262 variables (e.g., climate, CO₂, nitrogen deposition, fertilizer use, irrigation, and crop rotation).
263 For simulation scenarios S2 - S4, we assumed that a specific tillage practice was applied for all
264 the croplands across the basin over the study period. Comparing the four scenarios provides the
265 potential CWP change of adopting conservation tillage in the corn and soybean systems.

266 *<Insert Table 1>*

267 **3. Results**

268 **3.1 Historical changes in air temperature and precipitation in the ORB**

269 The ORB has been getting warmer and wetter during 1979-2018, with substantial interannual
270 variabilities in temperature and precipitation. The largest temperature increases occurred in the
271 periphery of the ORB region, including western Kentucky, southern and eastern Indiana, and
272 western Ohio (Fig. 3a). At the basin-level, air temperature has increased at a rate of 0.02 °C/year
273 since 1979 ($R^2 = 0.16$, $p < 0.05$; Fig. 3b). Relatively more precipitation increases occurred in the
274 center of the ORB, along both sides of the middle Ohio River, especially in southeastern Indiana
275 and northern/eastern Kentucky (Fig. 3c). The average precipitation increased at a rate of 3.9
276 mm/year since 1979 ($R^2 = 0.10$, $p < 0.05$; Fig. 3d). The ORB region is characterized by a wet
277 spring and dry autumn, with increased precipitation intensity and frequency in spring. Two
278 severe droughts (large increase in temperature and decrease in precipitation) occurred in 1987
279 and 2012. Two abnormally wet periods (large increase in precipitation with small temperature
280 change) were recorded in 1996 and 2018.

281

<Insert Figure 3>

282 **3.2 Tillage effects on GPP and ET over the ORB region**

283 In the ORB region, the mean annual GPP is 1264 ± 174 g C/m²/yr and 578 ± 150 g C/m²/yr for
284 corn and soybean, respectively (Figs. 4a, b). The spatial distribution patterns of GPP for corn and
285 soybean are similar to each other, with higher GPP in the northwest ORB region where
286 agriculture is the dominant land use. Compared to the baseline simulation (S1), tillage scenarios
287 (S2, S3, and S4) showed that the effect of tillage on GPP was negligible for both crops (Figs. 4c-
288 h). Nevertheless, NT and RT tended to have a slightly positive effect on GPP relative to CT.

289

<Insert Figure 4>

290 The spatial distribution patterns of annual ET for both crops showed an increasing trend from the
291 northeast toward the southwest region of the ORB (Figs. 5a, b). The average annual ET was 654
292 ± 43 mm/yr for corn and 454 ± 34 mm/yr for soybean. The sensitivity scenarios showed that CT
293 increased ET by $1.6 \pm 0.8\%$ in corn and $10.1 \pm 3.3\%$ in soybean (Figs. 5c, d; Table 2), while NT
294 decreased ET by $2.6 \pm 1.5\%$ in corn and $7.4 \pm 4.0\%$ in soybean (Figs. 5g, h), compared to the
295 baseline scenario (S1). Generally, the ET reduction under NT scenario was more pronounced in
296 the northwest of the ORB, where the annual ET was relatively low. The effect of RT on ET
297 relative to S1 was somewhat neutral ($-0.2 \pm 0.9\%$ and $1.4 \pm 2.9\%$ for corn and soybean,
298 respectively, Figs. 5e, f).

299

<Insert Figure 5>

300

<Insert Table 2>

301 **3.3 Tillage effects on CWP over the ORB region**

302 The baseline simulation (S1) showed that the mean annual CWP was $1.93 \pm 0.25 \text{ kg C/m}^3$ and
303 $1.28 \pm 0.36 \text{ kg C/m}^3$ for corn and soybean, respectively, across the ORB region during 1979 -
304 2018 (Figs. 6a, b). The spatial patterns for the annual CWP were similar for corn and soybean.
305 Areas with higher CWP occurred in the northwest section of ORB and decreased southeastward.
306 The sensitivity scenarios (S2, S3, and S4) revealed that the tillage-induced CWP change varied
307 among different tillage scenarios. Compared to the baseline scenario (S1), CT decreased the
308 mean annual CWP by $1.7 \pm 0.8\%$ for corn and $9.2 \pm 2.7\%$ for soybean (Figs. 6c, d; Table. 2),
309 while NT increased CWP by $2.8 \pm 1.6\%$ and $8.4 \pm 4.6\%$ for corn and soybean, respectively (Figs.
310 6g, h). The increase in CWP was more pronounced in the northern half of the ORB, where the
311 annual ET was relatively lower. However, the impact of RT on CWP was relatively neutral (0.1
312 $\pm 0.9\%$ and $-1.1 \pm 2.7\%$ for corn and soybean, respectively, Figs. 6e, f).

313 *<Insert Figure 6>*

314 The baseline temporal dynamics of the annual CWP showed a significant increasing trend
315 for soybean ($0.006 \text{ kg C/m}^3/\text{yr}$, $p < 0.01$, Fig. 7b) and corn ($0.004 \text{ kg C/m}^3/\text{yr}$, $p < 0.01$, Fig.7a).
316 Generally, throughout the simulation period, the NT scenario resulted in the highest annual CWP
317 for both crops in the ORB region ($1.98 \pm 0.07 \text{ kg C/m}^3$ and $1.37 \pm 0.09 \text{ kg C/m}^3$ for corn and
318 soybean, respectively). In comparison, the CT scenario led to the lowest annual CWP ($1.89 \pm$
319 0.08 kg C/m^3 and $1.13 \pm 0.08 \text{ kg C/m}^3$ for corn and soybean, respectively, Figs. 7a, b), despite
320 the variations in the annual CWP. No significant difference in the annual CWP was observed
321 between the RT and the baseline scenario.

322 *<Insert Figure 7>*

323 4. Discussion

324 4.1 Impacts of tillage management on crop GPP, ET, and CWP

325 Our results showed that, on average, across the ORB region, different tillage regimes had
326 indistinguishable effects on GPP for corn or soybean crops (Fig. 4). This is not surprising
327 considering that the ORB is often "water-rich" (Fig. 3d, Adler et al., 2003) with plentiful rainfall
328 as well as numerous major rivers and impoundments. Alterations in soil water dynamics caused
329 by different tillage methods would probably not limit water available for crops in the basin. Soil
330 and water conservation technologies do not necessarily lead to enhanced crop productivity
331 (Hellin and Schrader, 2003). Previous studies have suggested that, in comparison to humid
332 regions, dry areas where crop productivity is often limited by soil moisture could benefit more
333 from NT adoption (Huang et al., 2018; Pittelkow et al., 2015). A site-level study in Eastern and
334 Northern Ohio found, compared to CT, a slightly higher crop yield under conservation tillage at
335 a well-drained site, but no significant difference between tillage at a poorly drained site, despite
336 increased soil water retention under NT and RT (Kumar et al., 2012). Climate and soil may be
337 major factors influencing crop productivity response to tillage (Toliver et al., 2012). In Southern
338 Illinois, Kapusta et al. (1996) also observed no difference in corn yield among CT, NT, and RT
339 on a silt loam soil after 20 years under each tillage treatment. Moreover, similar GPP for wheat
340 between CT and NT systems was recently reported in the inland Pacific Northwest region with a
341 Mediterranean climate (Chi et al., 2016) and in the Southern Great Plains with a humid
342 subtropical climate (Kandel et al., 2020) using the eddy covariance method.

343 With respect to ET, our results are consistent with the current understanding that
344 conservation tillage decreases ET compared to CT (Fig. 5). NT and RT decreased ET by 2 ~ 4%
345 and 9 ~ 18% relative to CT in corn and soybean systems, respectively. These greater reductions

346 in evaporative water loss under NT would translate into more significant improvements in CWP,
347 the ratio of GPP to ET. The enhancement in CWP found under the NT and RT scenarios (Fig. 6)
348 was mainly due to decreased ET and minor changes in GPP. It should be noted that a noticeable
349 increase in CWP occurred in areas with relatively lower annual ET, and where there was a
350 greater reduction in ET under NT and RT compared to the areas with relatively higher ET (Fig. 5,
351 Table. 2). In addition, our results showed that NT and RT reduced evaporation compared to CT
352 (Fig. S1). They did not alter transpiration (Fig. S2), corresponding to the negligible distinctions
353 in GPP among different tillage scenarios. Surface residues create a physical barrier that reduces
354 evaporation and increases infiltration (Irmak et al., 2019). As a form of conservation tillage, NT
355 resulted in more crop residue coverage on the soil surface than CT and less evaporation. Besides,
356 tillage typically increases surface roughness, reduces albedo (Cierniewski et al., 2015), and
357 increases net absorption of solar radiation by the soil (Schwartz et al., 2010), hence fueling
358 evaporation. However, the effects of different tillage types on surface albedo and evaporation are
359 highly variable, depending on soil color, residues color, and residue incorporation. There is a
360 lack of representation of the direct effects of tillage on soil thermal properties (e.g., albedo) in
361 current modeling studies. Therefore, our results might underestimate or overestimate the
362 decrease in evaporation due to conservation tillage.

363 Soil water evaporation is generally not favorable for crop productivity, although
364 evaporation does slightly cool the surface microenvironment (Klocke et al., 2009), altering the
365 soil energy balance (O'Brien and Daigh, 2019). Thus, adopting conservation tillage can reduce
366 water loss via evaporation and make the soil more productive by maintaining soil moisture. One
367 concern regarding residue cover in conservation tillage systems is that it tends to retard seed
368 germination in the early spring due to the slow rate of soil warming (Blanco-Canqui and Lal,

369 2009) and could subsequently lead to reductions in crop productivity. For example, long-term
370 tillage studies in Illinois (Kapusta et al., 1996) and Indiana (Griffith et al., 1988) reported lower
371 corn plant populations under NT and RT systems than CT. However, these studies also suggested
372 that plant population differences among tillage systems did not translate into a yield deduction
373 when nitrogen fertilizer was applied. Our results revealed that GPP was also not affected by the
374 tillage regime at large spatial and temporal scales.

375 The present study also showed that the difference in CWP between NT and CT scenarios
376 was higher in soybean systems (~ 18%) than in corn systems (~ 5%, Fig. 6). In Minnesota, Tang
377 et al. (2015) observed similar results using eddy covariance measurement and MODIS products.
378 The greater response of soybean CWP could be due to its less water-efficient photosynthesis
379 pathway than corn (C3 vs. C4, Dietzel et al., 2016). It is worth noting that the soybean crop has a
380 much lower amount of residue than corn. Tillage after corn might lead to more residues and
381 exacerbate evaporation more than that after soybean. The increase in CWP in NT/RT soybean
382 was observed in rotations that soybean was sown after both corn and soybean. Considering that
383 most of the rotations were soybean after corn or/and corn after soybean (Table. S1), enhanced
384 soil water content due to NT and RT would increase soybean CWP more than corn CWP.

385 **4.2 Role of tillage management in the carbon and water cycles under climate change**

386 Increasing CWP under climate change will largely rely on management practices to reduce soil
387 water evaporation and shift water use to more transpiration (Hatfield and Dold, 2019). Soil
388 preparation plays a critical role in ensuring crop productivity and CWP in response to climate
389 change. Our results support the theory that conservation tillage can make agroecosystem less
390 susceptible to adverse impacts of climate change by partitioning more water into infiltration to
391 maintain soil moisture, thus potentially reducing crop water stress during drought conditions.

392 Besides, soils in the ORB are vulnerable to water erosion, particularly during heavy spring
393 rainstorms on croplands under CT systems (Van Pelt et al., 2017). Compared to CT, NT and RT
394 decreased surface runoff but increased subsurface drainage in the study region (Fig. 8). However,
395 the sum of runoff and drainage did not vary among different tillage scenarios. This finding is
396 consistent with Daryanto et al. (2017b). The shift in water fluxes (i.e., ET, runoff, and drainage)
397 among tillage systems further suggested the advantages of NT and RT in enhancing soil water
398 storage. Furthermore, it is generally perceived that NT and RT can reduce soil carbon loss
399 compared to CT, which helps maintain or build up soil carbon storage and improve soil structure
400 in the long run (Blanco-Canqui and Ruis, 2018). However, it should be noted that NT and RT
401 also increase subsurface drainage and potentially lead to more nutrient leaching. Daryanto et al.
402 (2017b) reported a greater loss of nitrate via leaching under NT than under CT despite similar
403 nitrate concentration under both systems. Similar results were also observed for dissolvable
404 phosphorus (Daryanto et al., 2017c). Considering the abundant rainfall amount in the ORB
405 region and the increasing trend in rainfall noted in the last several decades, there is a high
406 probability that nutrient leaching from croplands would be a growing concern in the region.
407 Therefore NT systems should be complemented with other measures to mitigate leaching loss.
408 For example, cover cropping and installation of water harvesting technologies (e.g., drainage
409 ditches with runoff filters, riparian buffers) can help increase available water for crops and lower
410 the risk of nutrient leaching (Daryanto et al., 2018; Liu et al., 2020).

411 *<Insert Figure 8>*

412 In addition, a recent study noted a declining trend in NT adoption across the US (including the
413 ORB) corn and soybean croplands since 2008, but increased adoption of RT (from 2006 to 2016)
414 and CT (from 2007 to 2016) (Yu et al., 2020). These trends can be ascribed to the release (2007

415 and 2016) of land previously enrolled in the Conservation Reserve Program (USDA, Farm
416 Service Agency 2019). Reports of increased resistance of weeds to herbicides may also play a
417 disincentivizing role in regard to NT adoption (Perry et al., 2016). Moreover, farmers tend to
418 make decisions based on many factors such as crop rotations, policies, and weather conditions.
419 Blanco-Canqui and Wortmann (2020) argued that occasionally tillage of cropland under NT
420 could be a potential solution to inadequate weed control and other risks associated with
421 continuous NT. However, more research is needed to identify options for optimizing the
422 environmental and cost-saving benefits of NT. It is essential to point out that our simulations
423 may represent the "best-case" NT vs "worst-case" CT scenarios, and therefore, the results should
424 be interpreted with caution. There is an urgent need for more spatio-temporally explicit data to
425 document agroecosystem-level water partitioning and further our ability to predict how tillage
426 regimes can help mitigate climate change impacts on crop productivity.

427 **5. Conclusions**

428 Process-based agroecosystem models are powerful tools that quantify large-scale carbon-water
429 interactions and explore associated underlying mechanisms under various tillage management
430 scenarios. This study offers the first attempt to quantify tillage effects on regional-scale CWP for
431 the two most important crops in the ORB. Model simulation results showed that if all the
432 croplands in the ORB region were under NT, the corn and soybean CWP would increase by 1-4%
433 and 4-13%, respectively. In contrast, adoption of CT practice would result in CWP decreases of
434 ~2% and ~9%, respectively. Our results indicate that conservation tillage can be a viable
435 approach to enhance CWP in corn and soybean cropping systems across the ORB. This benefit is
436 mainly due to lower water loss through non-beneficial evaporation under conservation tillage
437 systems. However, additional management practices and strategies are needed to decrease

438 nitrogen loss via leaching from croplands under NT. Future research should investigate the
439 synergic effects of these complementary measures and their potential to optimize the
440 environmental benefits of conservation tillage.

441

442 **Acknowledgments**

443 This work was supported by grants from the Alfred P. Sloan Foundation (G-2019-12468), the US
444 National Science Foundation (grant no. 1940696), and the National Institute of Food and
445 Agriculture (NIFA-USDA Hatch project 2352437000 and 2021-67013-33616). H.T.
446 acknowledged funding support from the US National Science Foundation (1903722) and the
447 Andrew Carnegie fellowship Program (G-F-19-56910). The statements made and views
448 expressed are solely the responsibility of the authors.

449

450 **References**

451 Abatzoglou, J.T., 2013. Development of gridded surface meteorological data for ecological
452 applications and modelling. *Int. J. Climatol.* 33, 121-131.

453 Adler, R.F., Huffman, G.J., Chang, A., Ferraro, R., Xie, P.P., Janowiak, J., Rudolf, B., Schneider,
454 U., Curtis, S., Bolvin, D., Gruber, A., 2003. The version-2 global precipitation climatology
455 project (GPCP) monthly precipitation analysis (1979–present). *J. Hydrometeorol.* 4(6),
456 1147-1167.

457 Ai, Z., Wang, Q., Yang, Y., Manevski, K., Yi, S., Zhao, X., 2020. Variation of gross primary
458 production, evapotranspiration and water use efficiency for global croplands. *Agric. For.*
459 *Meteorol.* 287, 107935.

- 460 Bai, X., Huang, Y., Ren, W., Coyne, M., Jacinthe, P.A., Tao, B., Hui, D., Yang, J., Matocha, C.,
461 2019. Responses of soil carbon sequestration to climate smart agriculture practices: A
462 meta-analysis. *Glob. Chang. Biol.* 25, 2591-2606.
- 463 Bandaru, V., West, T.O., Ricciuto, D.M., Izaurralde, R.C., 2013. Estimating crop net primary
464 production using national inventory data and MODIS-derived parameters. *ISPRS J.*
465 *Photogramm. Remote Sens.* 80, 61-71.
- 466 Blanco-Canqui, H., Lal, R., 2009. Crop residue removal impacts on soil productivity and
467 environmental quality. *Crit. Rev. Plant Sci.* 28(3), 139-163.
- 468 Blanco-Canqui, H., Ruis, S.J., 2018. No-tillage and soil physical environment. *Geoderma.* 326,
469 164-200.
- 470 Bluemling, B., Yang, H., Pahl-Wostl, C., 2007. Making water productivity operational– a
471 concept of agricultural water productivity exemplified as a wheat–maize cropping pattern
472 in the North China Plain. *Agric. Water Manage.* 91 (1–3), 11–23.
- 473 Brauman, K.A., Siebert, S., Foley, J.A., 2013. Improvements in crop water productivity increase
474 water sustainability and food security - a global analysis. *Environ. Res. Lett.* 8(2), 024030.
- 475 Busari, M.A., Kukal, S.S., Kaur, A., Bhatt, R., Dulazi, A.A., 2015. Conservation tillage impacts
476 on soil, crop and the environment. *Int. Soil Water Conserv. Res.* 3(2), 119-129.
- 477 Cantero-Martínez, C., Angás, P., Lampurlanés, J., 2007. Long-term yield and water use
478 efficiency under various tillage systems in Mediterranean rainfed conditions. *Ann. Appl.*
479 *Biol.* 150(3), 293-305.

480 Chi, J., Waldo, S., Pressley, S., O’Keeffe, P., Huggins, D., Stöckle, C., Pan, W.L., Brooks, E.,
481 Lamb, B., 2016. Assessing carbon and water dynamics of no-till and conventional tillage
482 cropping systems in the inland Pacific Northwest US using the eddy covariance method.
483 *Agric. For. Meteorol.* 218, 37-49.

484 Cierniewski, J., Karnieli, A., Kazmierowski, C., Krolewicz, S., Piekarczyk, J., Lewinska, K.,
485 Goldberg, A., Wesolowski, R., Orzechowski, M., 2015. Effects of soil surface
486 irregularities on the diurnal variation of soil broadband blue-sky albedo. *IEEE J. Selected*
487 *Topics Appl. Earth Obser. Remote Sens.* 8, 493–502.

488 Conservation Tillage Information Center (CTIC), 2018. The Operational Tillage Information
489 System (OpTIS). https://www.ctic.org/OpTIS_tabular_query (accessed 26 August 2019).

490 Daryanto, S., Wang, L., Jacinthe, P.A., 2017a. Global synthesis of drought effects on cereal,
491 legume, tuber and root crops production: A review. *Agric. Water Manag.* 179, 18-33.

492 Daryanto, S., Wang, L., Jacinthe, P.A., 2017b. Impacts of no-tillage management on nitrate loss
493 from corn, soybean and wheat cultivation: A meta-analysis. *Sci. Rep.* 7(1), 12117.

494 Daryanto, S., Wang, L. and Jacinthe, P.A. (2017), Meta-Analysis of Phosphorus Loss from No-
495 till Soils. *J. Environ. Qual.*, 46: 1028-1037.

496 Daryanto, S., Fu, B., Wang, L., Jacinthe, P.A., Zhao, W., 2018. Quantitative synthesis on the
497 ecosystem services of cover crops. *Earth-Sci. Rev.* 185, 357-373.

498 Dietzel, R., Liebman, M., Ewing, R., Helmers, M., Horton, R., Jarchow, M., Archontoulis, S.,
499 2016. How efficiently do corn- and soybean- based cropping systems use water? A
500 systems modeling analysis. *Glob. Chang. Biol.* 22(2), 666-681.

501 Drum, R.G., Noel, J., Kovatch, J., Yeghiazarian, L., Stone, H., Stark, J., Kirshen, P., Best, E.,
502 Emery, E., Trimboli, J., Arnold, J., Raff, D., 2017. Ohio River Basin–Formulating Climate
503 Change Mitigation/Adaptation Strategies Through Regional Collaboration with the ORB
504 Alliance, May 2017. Civil Works Technical Report, CWTS 2017-01, U.S. Army Corps of
505 Engineers, Institute for Water Resources: Alexandria, VA.

506 Franklin, D.H, Bergtold, Jason, 2020. Conservation tillage systems: history, the future and
507 benefits, in Bergtold, J., Sailus, M. (Eds.), Conservation Tillage Systems in the Southeast:
508 Production, Profitability and Stewardship. Sustainable Agriculture Research and Education
509 (SARE). pp. 19-28.

510 Griffith, D., Kladivko, E., Mannering, J.V., West, T., Parsons, S., 1988. Long-term tillage and
511 rotation effects on corn growth and yield on high and low organic matter, poorly drained
512 soils. *Agron. J.* 80(4), 599-605.

513 Guan, D., Zhang, Y., Al-Kaisi, M.M., Wang, Q., Zhang, M., Li, Z., 2015. Tillage practices effect
514 on root distribution and water use efficiency of winter wheat under rain-fed condition in
515 the North China Plain. *Soil Tillage Res.* 146, 286-295.

516 Hatfield, J.L., Dold, C., 2019. Water-Use Efficiency: Advances and Challenges in a Changing
517 Climate. *Front. Plant Sci.* 10, 103.

518 Hellin, J., Schrader, K., 2003. The case against direct incentives and the search for alternative
519 approaches to better land management in Central America. *Agric. Ecosyst. Environ.* 99(1-
520 3), 61-81.

521 Hember, R.A., 2018. Spatially and temporally continuous estimates of annual total nitrogen
522 deposition over North America, 1860–2013. *Data Brief* 17, 134-140.

523 Holland, J., 2004. The environmental consequences of adopting conservation tillage in Europe:
524 reviewing the evidence. *Agric. Ecosyst. Environ.* 103(1), 1-25.

525 Huang, Y., Ren, W., Wang, L., Hui, D., Grove, J.H., Yang, X., Tao, B., Goff, B., 2018.
526 Greenhouse gas emissions and crop yield in no-tillage systems: A meta-analysis. *Agric.*
527 *Ecosyst. Environ.* 268, 144-153.

528 Huang Y., Ren, W., Grove, J.H., Poffenbarger, H., Jacobson, K., Tao, B., Zhu, X., McNear, D.,
529 2020. Assessing synergistic effects of no-tillage and cover crops on soil carbon dynamics
530 in a long-term maize cropping system under climate change. *Agric. For. Meteorol.* 291,
531 108090.

532 Irmak, S., Kukal, M.S., Mohammed, A.T., Djaman, K., 2019. Disk-till vs. no-till maize
533 evapotranspiration, microclimate, grain yield, production functions and water productivity.
534 *Agric. Water Manag.* 216, 177-195.

535 Jabro, J.D., Stevens, W.B., Iverson, W.M., Evans, R.G., Allen, B.L., 2014. Crop water
536 productivity of sugarbeet as affected by tillage. *Agron. J.* 106(6), 2280-2286.

537 Kandel, T.P., Gowda, P.H., Northup, B.K., 2020. Influence of tillage systems, and forms and
538 rates of nitrogen fertilizers on CO₂ and N₂O fluxes from winter wheat cultivation in
539 Oklahoma. *Agron.* 10(3), 320.

540 Kapusta, G., Krausz, R.F., Matthews, J.L., 1996. Corn yield is equal in conventional, reduced,
541 and no tillage after 20 years. *Agron. J.* 88(5), 812-817.

542 Klocke, N., Currie, R., Aiken, R., 2009. Soil water evaporation and crop residues. *Trans.*
543 *ASABE* 52, 103–110.

- 544 Kumar, S., Kadono, A., Lal, R., Dick, W., 2012. Long-term no-till impacts on organic carbon
545 and properties of two contrasting soils and corn yields in Ohio. *Soil Sci. Soc. Am. J.* 76(5),
546 1798-1809.
- 547 Lal, R., Delgado, J., Groffman, P., Millar, N., Dell, C., Rotz, A., 2011. Management to mitigate
548 and adapt to climate change. *J. Soil Water Conserv.* 66(4), 276-285.
- 549 Lal, R., Logan, T.J., Eckert, D.J., Dick, W.A., Shipitalo, M.J., 2017. Conservation tillage in the
550 corn belt of the United States, in Carter, M.R. (Ed.), *Conservation Tillage in Temperate*
551 *Agroecosystems*. CRC Press Inc., Boca Raton, FL, USA, pp. 73-114.
- 552 Li, N., Zhou, C., Sun, X., Jing, J., Tian, X., Wang, L., 2018. Effects of ridge tillage and mulching
553 on water availability, grain yield, and water use efficiency in rain-fed winter wheat under
554 different rainfall and nitrogen conditions. *Soil Tillage Res.* 179, 86-95.
- 555 Li, Y., Guan, K., Schnitkey, G. D., DeLucia, E., Peng, B., 2019. Excessive rainfall leads to
556 maize yield loss of a comparable magnitude to extreme drought in the United States. *Glob.*
557 *Chang. Biol.* 25(7), 2325-2337.
- 558 Li, Z., Liu, S., Tan, Z., Bliss, N.B., Young, C.J., West, T.O., Ogle, S.M., 2014. Comparing
559 cropland net primary production estimates from inventory, a satellite-based model, and a
560 process-based model in the Midwest of the United States. *Ecol. Modell.* 277, 1-12.
- 561 Liu, S., Zhang, X.Y., Yang, J., Drury, C.F., 2013. Effect of conservation and conventional tillage
562 on soil water storage, water use efficiency and productivity of corn and soybean in
563 Northeast China. *Acta Agric. Scand. B Soil Plant Sci.* 63(5), 383-394.

564 Liu, Y., Song, W., 2020. Modelling crop yield, water consumption, and water use efficiency for
565 sustainable agroecosystem management. *J. Clean. Prod.* 253, 119940.

566 Lu, X., Zhuang, Q., 2010. Evaluating evapotranspiration and water-use efficiency of terrestrial
567 ecosystems in the conterminous United States using MODIS and AmeriFlux data. *Remote*
568 *Sens. Environ.* 114(9), 1924-1939.

569 Lutz, F., Herzfeld, T., Heinke, J., Rolinski, S., Schaphoff, S., Bloh, W.V., Stoorvogel, J.J.,
570 Müller, C., 2019. Simulating the effect of tillage practices with the global ecosystem model
571 LPJmL (version 5.0-tillage). *Geosci. Model Dev.* 12(6), 2419-2440.

572 O'Brien, P.L., Daigh, A.L., 2019. Tillage practices alter the surface energy balance—A review.
573 *Soil Tillage Res.* 195, 104354.

574 Ordóñez, R.A., Archontoulis, S.V., Martinez-Feria, R., Hatfield, J.L., Wright, E.E., Castellano,
575 M.J., 2020. Root to shoot and carbon to nitrogen ratios of maize and soybean crops in the
576 US Midwest. *Eur. J. Agron.* 120, 126130.

577 Panagopoulos, Y., Gassman, P.W., Arritt, R.W., Herzmann, D.E., Campbell, T.D., Valcu, A., Jha,
578 M.K., Kling, C.L., Srinivasan, R., White, M., Arnold, J.G., 2015. Impacts of climate
579 change on hydrology, water quality and crop productivity in the Ohio-Tennessee River
580 Basin. *Int. J. Agric. Biol. Eng.* 8(3), 36-53.

581 Perry, C., 2007. Efficient irrigation; inefficient communication; flawed recommendations. *Irrig.*
582 *Drain.* 56 (4), 367–378.

583 Perry, E. D., Ciliberto, F., Hennessy, D. A., Moschini, G., 2016. Genetically engineered crops
584 and pesticide use in US maize and soybeans. *Sci. Adv.*, 2(8), e1600850.

585 Pervez M. S., Brown J.F., 2010. Mapping irrigated lands at 250-m scale by merging MODIS data
586 and National Agricultural Statistics. *Remote Sens.* 2(10), 2388-2412.

587 Phillips, R.E., Thomas, G.W., Blevins, R.L., Frye, W.W., Phillips, S.H., 1980. No-tillage
588 agriculture. *Science* 208(4448), 1108-1113.

589 Pittelkow, C.M., Liang, X., Linquist, B.A., Van Groenigen, K.J., Lee, J., Lundy, M.E., Van
590 Gestel, N., Six, J., Venterea, R.T., Van Kessel, C., 2015. Productivity limits and potentials
591 of the principles of conservation agriculture. *Nature* 517(7534), 365.

592 Prince, S.D., Haskett, J., Steininger, M., Strand, H., Wright, R., 2001. Net primary production of
593 US Midwest croplands from agricultural harvest yield data. *Ecol. Appl.* 11(4), 1194-1205.

594 Ren, W.E.I., Tian, H., Xu, X., Liu, M., Lu, C., Chen, G., Melillo, J., Reilly, J., Liu, J., 2011.
595 Spatial and temporal patterns of CO₂ and CH₄ fluxes in China's croplands in response to
596 multifactor environmental changes. *Tellus B Chem. Phys. Meteorol.* 63, 222-240.

597 Ren, W., Tian, H., Tao, B., Huang, Y., Pan, S., 2012. China's crop productivity and soil carbon
598 storage as influenced by multifactor global change. *Glob. Chang. Biol.* 18, 2945-2957.

599 Ren, W., Tian, H., Cai, W.J., Lohrenz, S.E., Hopkinson, C.S., Huang, W.J., Yang, J., Tao, B.,
600 Pan, S., He, R., 2016. Century-long increasing trend and variability of dissolved organic
601 carbon export from the Mississippi River basin driven by natural and anthropogenic
602 forcing. *Global Biogeochem. Cycles* 30 (9), 1288-1299.

603 Ren, W., Banger, K., Tao, B., Yang, J., Huang, Y., Tian, H., 2020. Global pattern and change of
604 cropland soil organic carbon during 1901-2010: Roles of climate, atmospheric chemistry,
605 land use and management, *Geogr. Sustain.* 1(1):59-69.

606 Santhi, C., Kannan, N., White, M., Di Luzio, M., Arnold, J., Wang, X., Williams, J., 2014. An
607 integrated modeling approach for estimating the water quality benefits of conservation
608 practices at the river basin scale. *J. Environ. Qual.* 43(1), 177-198.

609 Schilling, K. E., Wolter, C. F., McLellan, E., 2015. Agro-hydrologic landscapes in the upper
610 Mississippi and Ohio River basins. *Environ. Manag.* 55(3), 646-656.

611 Schwartz, R.C., Baumhardt, R.L., Evett, S.R., 2010. Tillage effects on soil water redistribution
612 and bare soil evaporation throughout a season. *Soil Tillage Res.* 110(2), 221-229. doi:
613 <https://doi.org/10.1016/j.still.2010.07.015>

614 Shekhar, A., Shapiro, C.A., 2019. What do meteorological indices tell us about a long-term
615 tillage study? *Soil Tillage Res.* 193, 161-170.

616 Strudley, M.W., Green, T.R., Ascough II, J.C., 2008. Tillage effects on soil hydraulic properties
617 in space and time: State of the science. *Soil Tillage Res.* 99(1), 4-48.

618 Su, Z., Zhang, J., Wu, W., Cai, D., Lv, J., Jiang, G., Huang, J., Gao, J., Hartmann, R., Gabriels,
619 D., 2007. Effects of conservation tillage practices on winter wheat water-use efficiency and
620 crop yield on the Loess Plateau, China. *Agric. Water Manag.* 87(3), 307-314.

621 Tang, X., Ding, Z., Li, H., Li, X., Luo, J., Xie, J., Chen, D., 2015. Characterizing ecosystem
622 water-use efficiency of croplands with eddy covariance measurements and MODIS
623 products. *Ecol. Eng.* 85, 212-217.

624 Tian, H., Chen, G., Liu, M., Zhang, C., Sun, G., Lu, C., Xu, X., Ren, W., Pan, S., Chappelka, A.,
625 2010. Model estimates of net primary productivity, evapotranspiration, and water use

626 efficiency in the terrestrial ecosystems of the southern United States during 1895–2007.
627 For. Ecol. Manag. 259(7), 1311-1327.

628 Tian, H., Lu, C., Pan, S., Yang, J., Miao, R., Ren, W., Yu, Q., Fu, B., Jin, F., Lu, Y., Melillo, J.,
629 Ouyang, Z., Palm, C., Reilly, J., 2018. Optimizing resource use efficiencies in the food–
630 energy–water nexus for sustainable agriculture: from conceptual model to decision support
631 system. *Curr. Opin. Environ. Sustain.* 33, 104-113.

632 Tian, H., Lu, C., Yang, J., Banger, K., Huntzinger, D.N., Schwalm, C.R., Michalak, A.M.,
633 Cook, R., Ciais, P., Hayes, D., Huang, M., Ito, A., Jain, A.K., Lei, H., Mao, J., Pan, S., Post,
634 W.M., Peng, S., Poulter, B., Ren, W., Ricciuto, D., Schaefer, K., Shi, X., Tao, B., Wang,
635 W., Wei, Y., Yang, Q., Zhang, B., Zeng, N.C.G.B., 2015. Global patterns and controls of
636 soil organic carbon dynamics as simulated by multiple terrestrial biosphere models: current
637 status and future directions. *Glob. Biogeochem. Cycles.* 29(6), 775-792.

638 Toliver, D.K., Larson, J.A., Roberts, R.K., English, B.C., De La Torre Ugarte, D.G., West, T.O.,
639 2012. Effects of no-till on yields as influenced by crop and environmental factors. *Agron. J.*
640 104(2), 530-541.

641 Turner, D.P., Ritts, W.D., Cohen, W.B., Maeirsperger, T.K., Gower, S.T., Kirschbaum, A.A.,
642 Running, S.W., Zhao, M., Wofsy, S.C., Dunn, A.L., Law, B.E., 2005. Site-level evaluation
643 of satellite-based global terrestrial gross primary production and net primary production
644 monitoring. *Glob. Chang. Biol.* 11(4), 666-684.

645 Turner, D.P., Ritts, W.D., Cohen, W.B., Gower, S.T., Running, S.W., Zhao, M., Costa, M.H.,
646 Kirschbaum, A.A., Ham, J.M., Saleska, S.R., Ahl, D.E., 2006. Evaluation of MODIS NPP
647 and GPP products across multiple biomes. *Remote Sens. Environ.* 102(3-4), 282-292.

648 USDA Natural Resources Conservation Service and University of Wisconsin—Extension. 2019.
649 Residue management choices: a guide to managing crop residues in corn and soybeans.

650 Van Halsema, G. E., Vincent, L., 2012. Efficiency and productivity terms for water management:
651 A matter of contextual relativism versus general absolutism. *Agric. Water Manag.* 108, 9-
652 15.

653 Van Pelt, R.S., Hushmurodov, S.X., Baumhardt, R.L., Chappell, A., Nearing, M.A., Polyakov,
654 V.O., Strack, J.E., 2017. The reduction of partitioned wind and water erosion by
655 conservation agriculture. *Catena* 148, 160-167.

656 Wuebbles, D. J., Fahey, D. W., Hibbard, K. A., Dokken, D. J., Stewart, B. C., Maycock, T. K.,
657 2017. Climate science special report: Fourth national climate assessment, Vol. I.
658 Washington, DC: U.S. Global Change Research Program.

659 Yang, X., Zheng, L., Yang, Q., Wang, Z., Cui, S., Shen, Y., 2018. Modelling the effects of
660 conservation tillage on crop water productivity, soil water dynamics and
661 evapotranspiration of a maize-winter wheat-soybean rotation system on the Loess Plateau
662 of China using APSIM. *Agric. Syst.* 166, 111-123.

663 Yang, Y., Ren, W., Tao, B., Ji, L., Liang, L., Ruane, A.C., Fisher, J.B., Liu, J., Sama, M., Li, Z.,
664 Tian, Q., 2020. Characterizing spatiotemporal patterns of crop phenology across North
665 America during 2000-2016 using satellite imagery and agricultural survey data. *ISPRS J.*
666 *Photogramm. Remote Sens.* 170, 156-173.

667 Yu, Z., Lu, C., Hennessy, D. A., Feng, H., Tian, H., 2020. Impacts of tillage practices on soil
668 carbon stocks in the US corn-soybean cropping system during 1998 to 2016. *Environ. Res.*
669 *Lett.* 15(1), 014008.

670 Zhang, J., Tian, H., Yang, J., Pan, S., 2018. Improving representation of crop growth and yield in
671 the dynamic land ecosystem model and its application to China. *J. Adv. Model. Earth Syst.*
672 10 (7), 1680-1707.

673

674 Table 1. Simulation design in this study.

Scenarios	Abbr	Drivers used	
		Tillage	Others ^a
Historical varying tillage	S1	1979 - 2018	Varying
Conventional tillage	S2	1979 ^b	Varying
Reduced tillage	S3	1979 ^c	Varying
No-tillage	S4	1979 ^d	Varying

675 Note: ^a Others include climate data (e.g., air temperature, precipitation, and radiation from 1979
676 to 2018), agricultural nitrogen fertilizer (i.e., nitrogen fertilizer from 1979 to 2018), and
677 atmospheric conditions (i.e., CO₂ and N deposition from 1979 to 2018); ^b Tillage intensity across
678 the ORB for the entire period was consistent as conventional tillage (CT); ^c Tillage intensity
679 across the ORB for the entire period was consistent as reduced tillage (RT); ^d Tillage intensity
680 across the ORB for the entire period was consistent as no-tillage (NT).

681

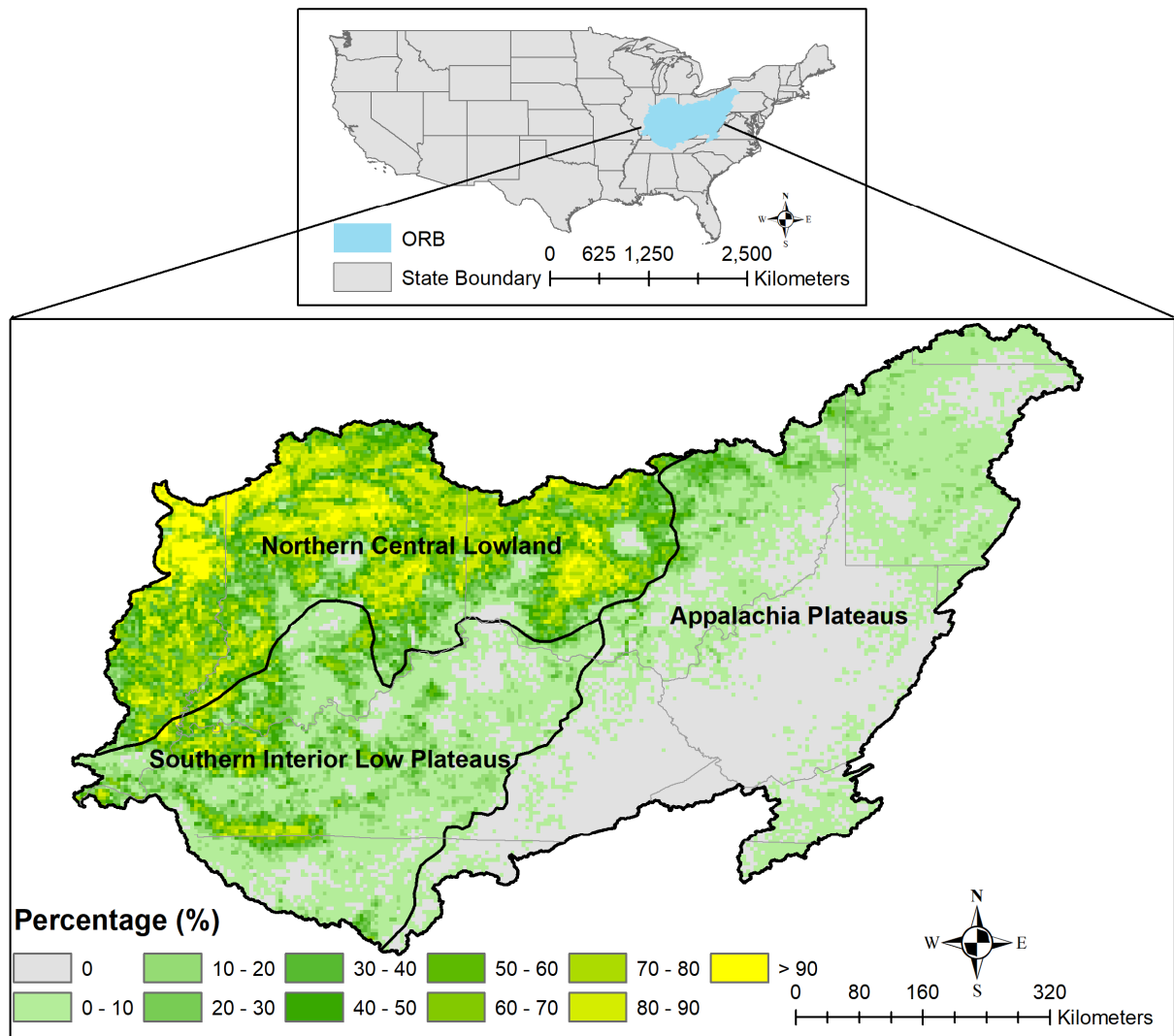
682

683 Table 2. Regional summary of the percentage change from the simulation scenario S1 (GPP, ET, and CWP) owing to CT, RT, and NT.

	Region	Corn			Soybean		
		CT	RT	NT	CT	RT	NT
Δ GPP (%)	NCL*	-0.04±0.02	0.01±0.02	0.08±0.03	-0.03±1.45	0.06±0.12	0.03±0.18
	SILP	-0.03±0.15	-0.01±0.04	0.02±0.08	0.42±1.08	0.54±1.08	0.62±1.10
	AP	-0.05±0.06	0.01±0.05	0.08 ± 0.08	-0.08±0.48	0.11±0.47	0.23±0.48
	ORB	-0.05±0.09	0.00±0.04	0.06±0.07	0.10±0.72	0.23±0.71	0.27±0.74
Δ ET (%)	NCL	1.39±0.50	-0.37±0.5	-2.83±0.70	11.28±2.47	1.27±1.49	-8.13±1.82
	SILP	1.59±0.49	0.39±0.37	-1.38±0.56	9.00±3.33	3.04±2.52	-3.91±2.63
	AP	2.04±1.17	-0.46±1.32	-3.71±1.86	9.67±3.82	-1.12±3.72	-11.44±4.42
	ORB	1.63±0.80	-0.17±0.88	-2.64±1.45	10.15±3.27	1.35±2.89	-7.40±3.98
Δ CWP (%)	NCL	-1.43±0.50	0.37±0.52	3.00±0.76	-10.29±2.04	-1.26±1.47	8.90±2.08
	SILP	-1.63±0.51	-0.42±0.38	1.43 ± 0.61	-7.96±2.56	-2.43±1.91	4.82±2.35
	AP	-2.08±1.15	0.47±1.38	3.96 ± 2.11	-9.01±3.19	1.30±3.95	13.31±5.83
	ORB	-1.68±0.79	0.14±0.93	2.77±1.62	-9.22±2.71	-1.14±2.72	8.38±4.55

684 * NCL: Northern Central Lowland; SILP: Southern Interior Low Plateaus; AP: Appalachia Plateaus; ORB: whole Ohio River Basin.

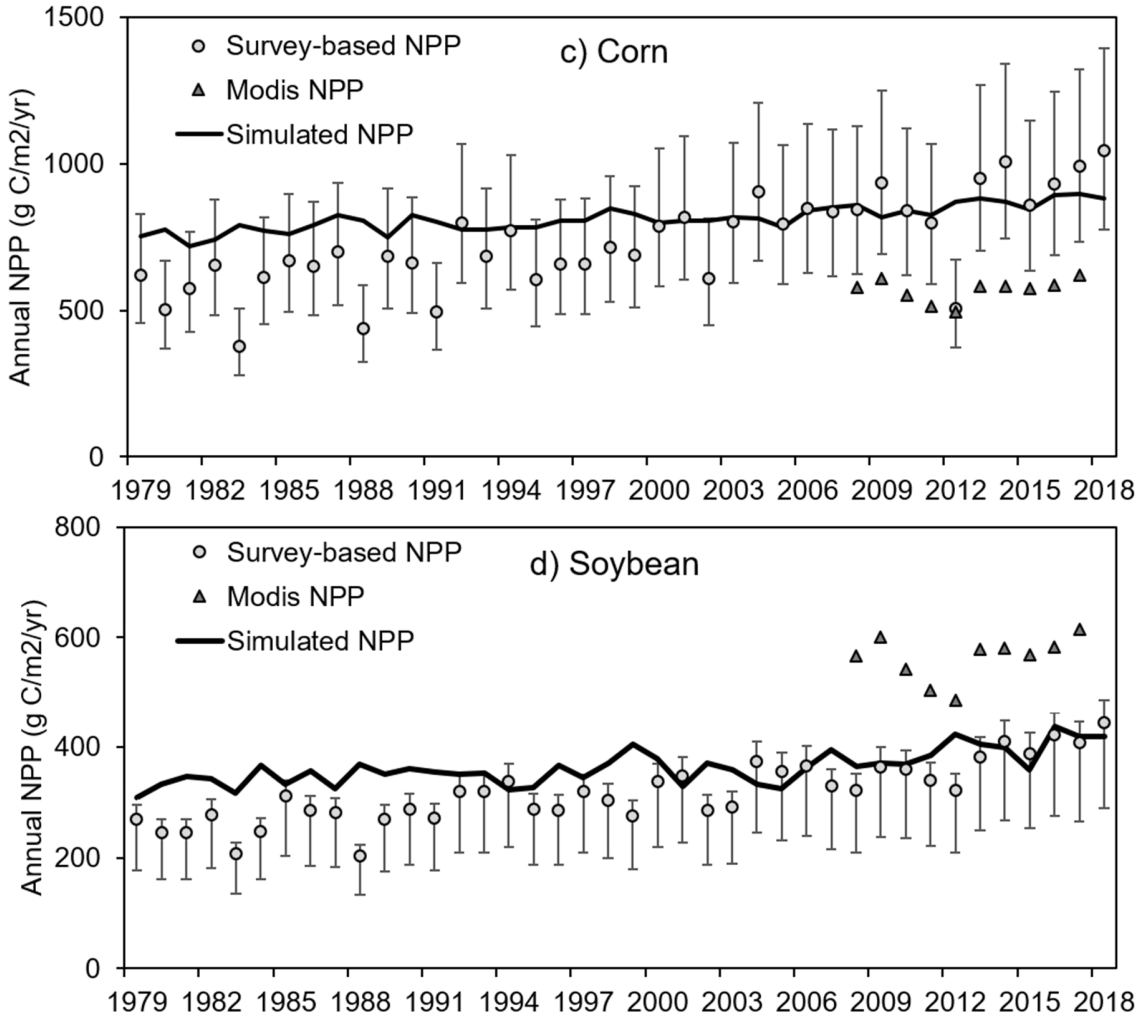
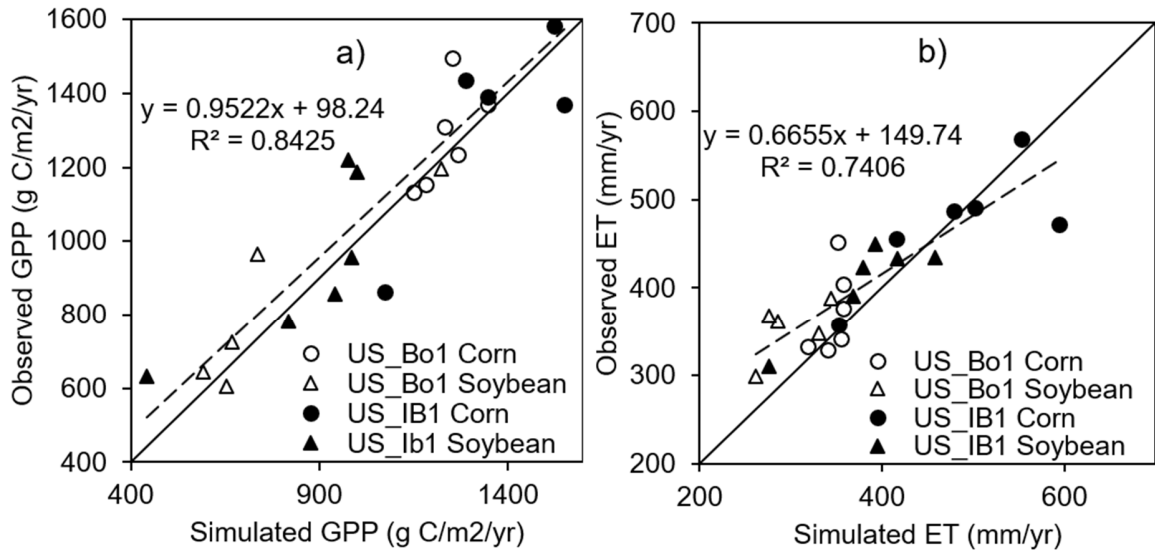
685



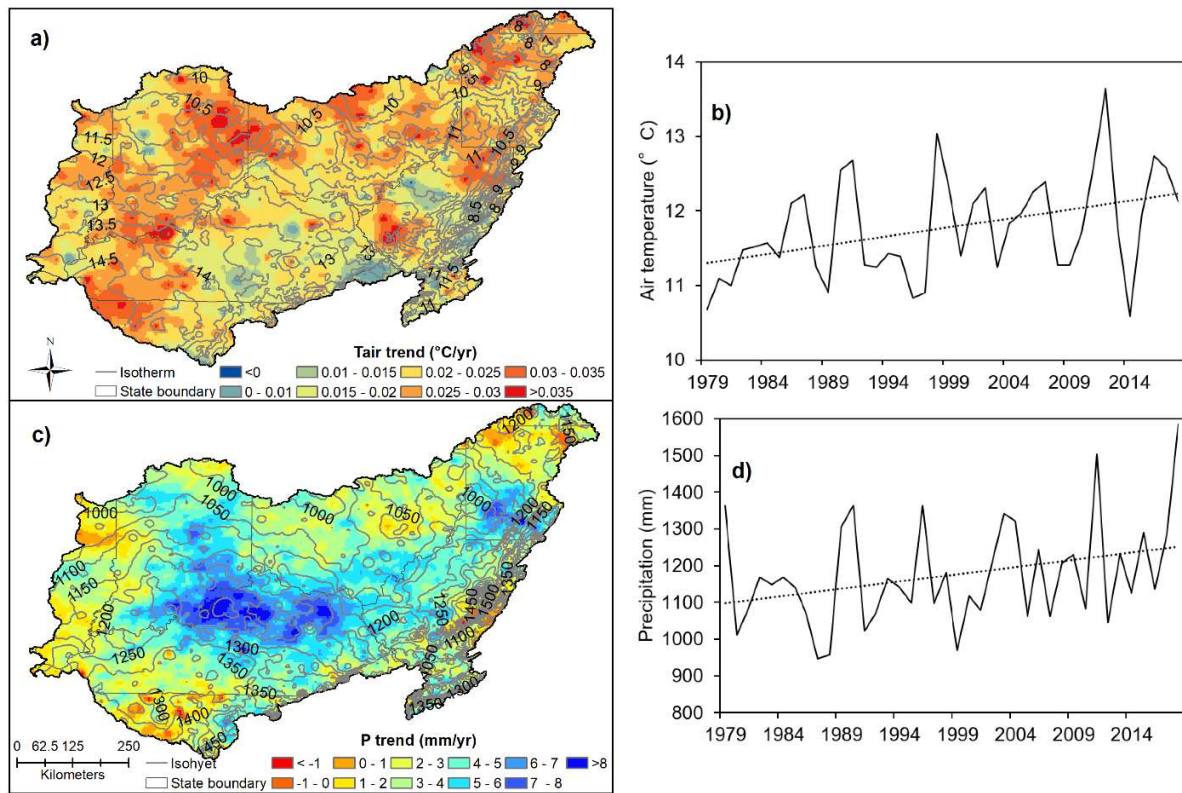
686

687 Figure 1. Location of the Ohio River Basin and percentage of cropland are for the eight rotation
688 types at a spatial resolution of 4-km. Subregions are based on the physiographic divisions of the
689 conterminous US.

690



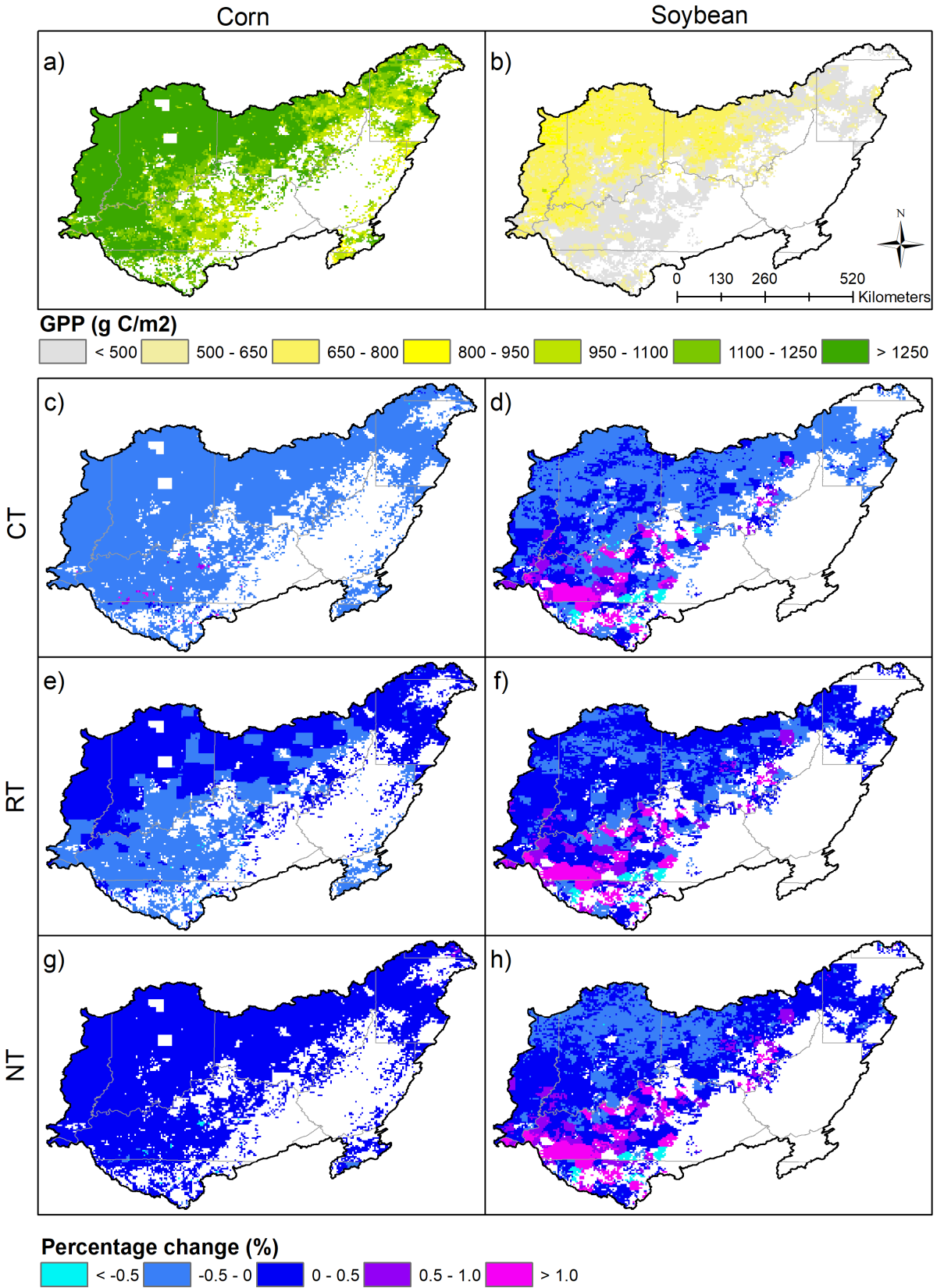
692 Figure 2. Comparison of model estimated and observed gross primary productivity (GPP; a) and
693 evapotranspiration (ET; b) for corn and soybean at sites US-BO1 (1997-2006) and US-IB1
694 (2006-2017) (dashed line is the regression of observed data and modeled results. The solid line is
695 the 1:1 line). Comparisons of basin-level annual NPP derived from USDA survey, MODIS NPP
696 datasets, and model simulations for corn (c) and soybean (d). Error bars represent the upper and
697 lower limits of yield-derived NPP based on the parameter ranges.



698

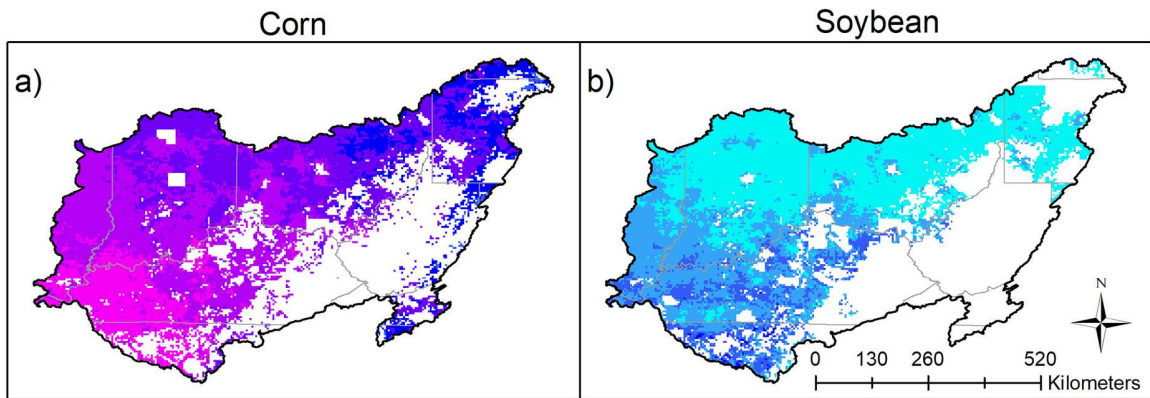
699 Figure 3. Spatial and temporal change of annual (a, b) air temperature, (c, d) precipitation
 700 between 1979 and 2018. Contour lines in a and b represent isotherm and isohyet, respectively.

701

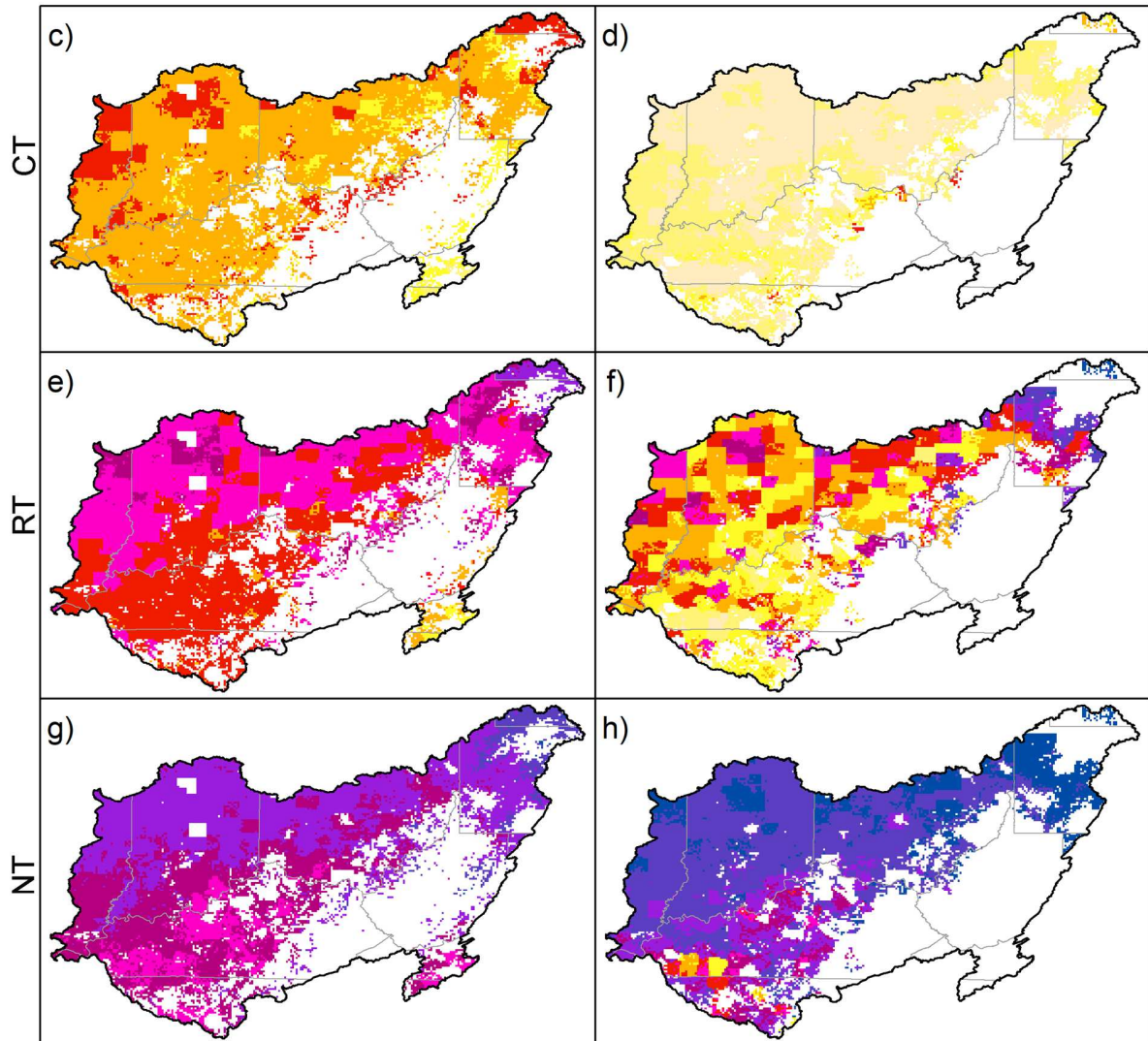
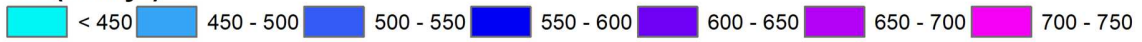


703 Figure 4. Spatial distribution of the mean annual (1979 - 2018) gross primary productivity (GPP)
704 in the ORB region from simulation scenario S1 (a, b), and the percentage change from the
705 simulation scenario S1 GPP owing to CT (c, d), RT (e, h), and NT (g, h). The left panel is for
706 corn, and the right panel is for soybean.

707



ET (mm/yr)



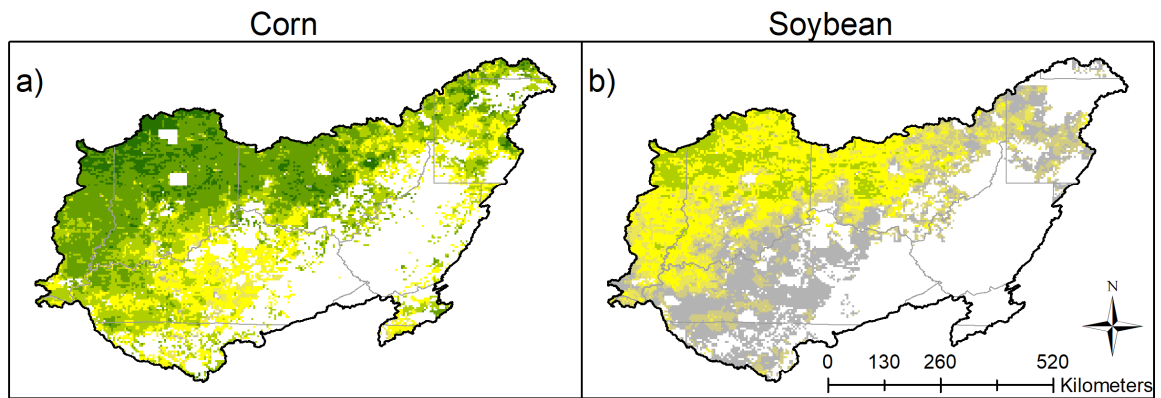
Percentage change (%)



709 Figure 5. Spatial distribution of the mean annual (1979 - 2018) evapotranspiration (ET) in the
710 ORB region from simulation scenario S1 (a, b), and the percentage change from the simulation
711 scenario S1 ET owing to CT (c, d), RT (e, h), and NT (g, h). The left panel is for corn, and the
712 right panel is for soybean.

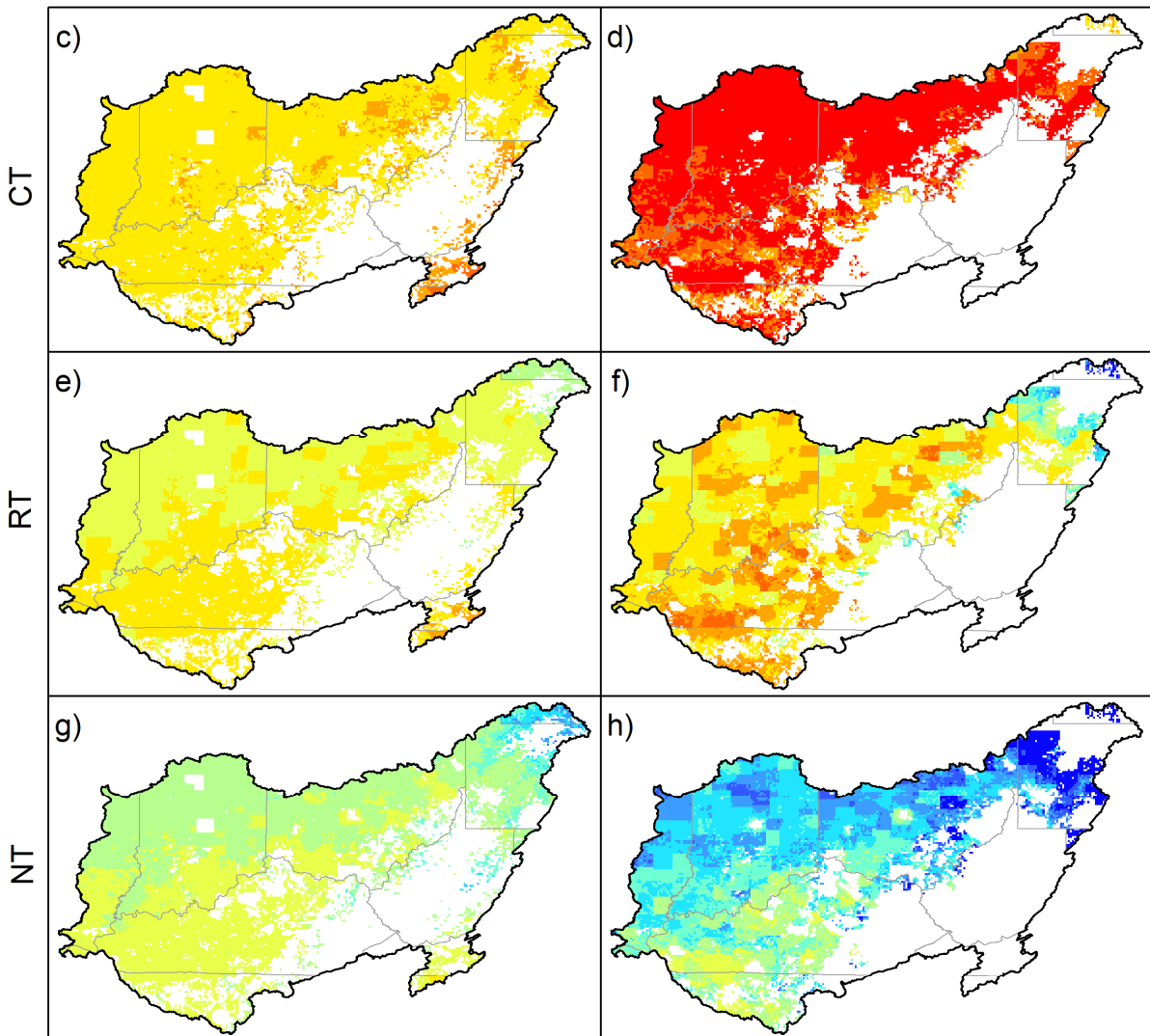
713

714



CWP (Kg C/m3)

< 1.0	1.0 - 1.25	1.25 - 1.5	1.5 - 1.75	1.75 - 2.0	2.0 - 2.25	> 2.25
-------	------------	------------	------------	------------	------------	--------

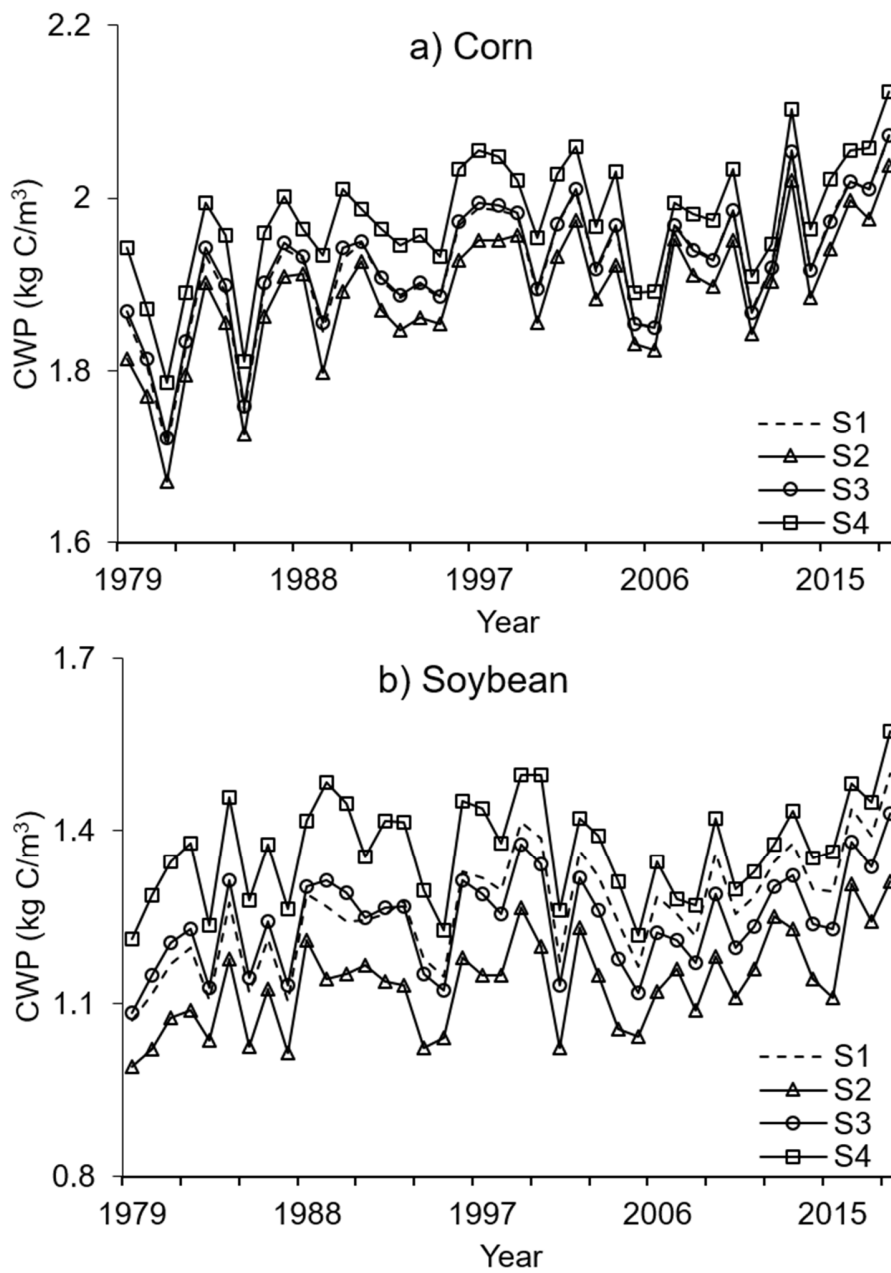


Percentage change (%)

< -7.5	-5.0 - -2.5	0 - 2.5	5.0 - 7.5	10.0 - 12.5	15.0 - 17.5
-7.5 - -5.0	-2.5 - 0	2.5 - 5.0	7.5 - 10.0	12.5 - 15.0	

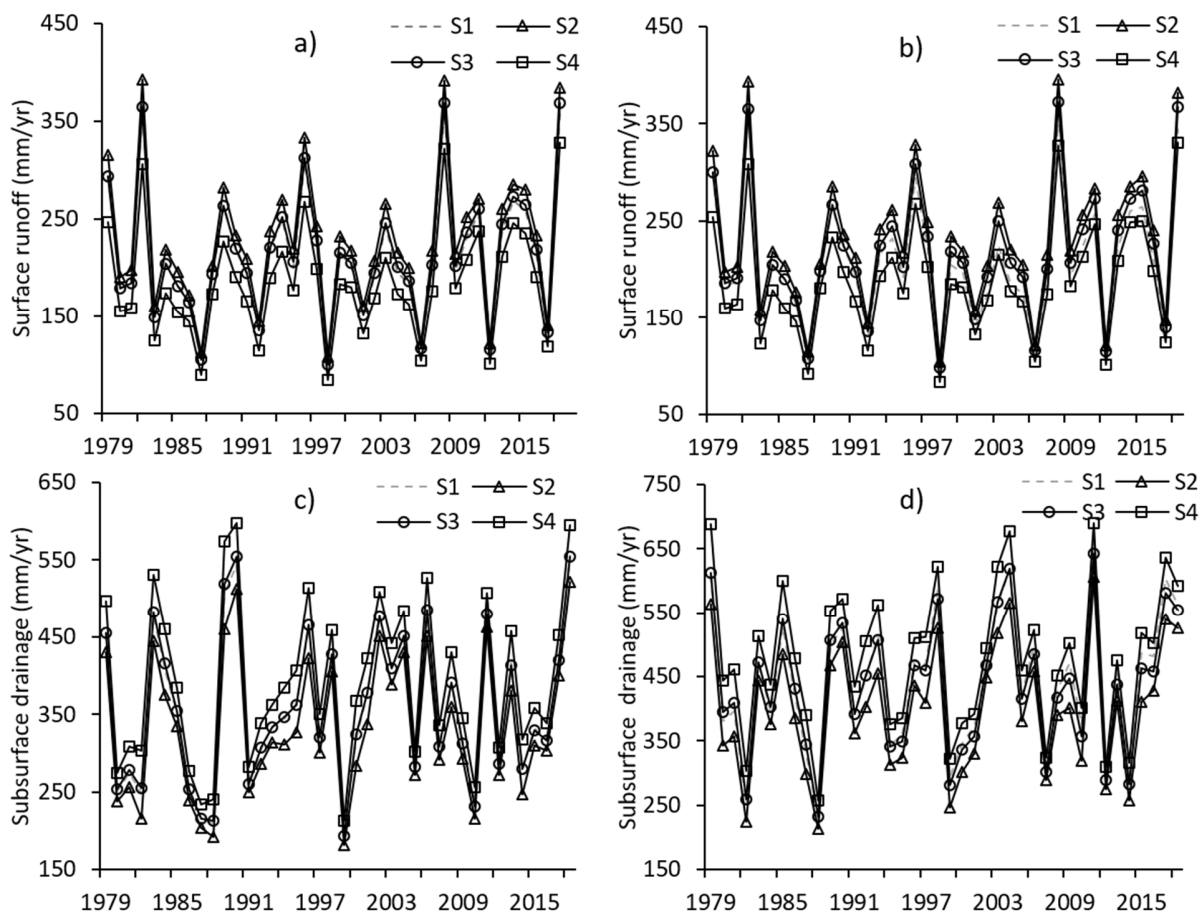
716 Figure 6. Spatial distribution of the mean annual (1979 - 2018) crop water productivity (CWP) in
 717 the ORB region from simulation scenario S1 (a, b), and the percentage change from the
 718 simulation scenario S1 CWP owing to CT (c, d), RT (e, h), and NT (g, h). The left panel is for
 719 corn , and the right panel is for soybean.

720



721

722 Figure 7. Temporal changes in crop water productivity (CWP) under different simulation
 723 scenarios for corn (a) and soybean (b) over the ORB region. S1, S2, S3, and S4 are different
 724 simulation scenarios as shown in Table 1.



725
 726 Figure 8. Temporal changes in surface runoff (a, b) and subsurface drainage (c, d) under different
 727 simulation scenarios for corn (left panel) and soybean (right panel) over the ORB region. S1, S2,
 728 S3, and S4 are different simulation scenarios as shown in Table 1.

729

730